

# 1,3-Bis(thiophosphinoyl)indene: A Unique and Versatile Scaffold for Original Polymetallic Complexes

Noel Nebra,<sup>†</sup> Nathalie Saffon,<sup>‡</sup> Laurent Maron,<sup>\*,§</sup> Blanca Martin–Vaca,<sup>\*,†</sup> and Didier Bourissou<sup>\*,†</sup>

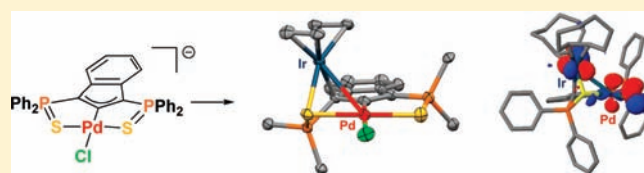
<sup>†</sup>Université de Toulouse, UPS, LHFA, 118 Route de Narbonne, and CNRS, LHFA UMR 5069, F-31062 Toulouse, France

<sup>‡</sup>Université de Toulouse, UPS, Institut de Chimie de Toulouse, FR2599, 118 Route de Narbonne, F-31062 Toulouse, France

<sup>§</sup>Université Paul Sabatier and INSA, UPS, LPCNO, 135 Avenue de Rangueil, and CNRS, LPCNO UMR 5215, 31077 Toulouse, France

**S** Supporting Information

**ABSTRACT:** The coordination of tridentate ligands featuring lateral coordination sites prone to acting as bridging ligands was explored with the aim of obtaining original polymetallic species in a straightforward and controlled manner. Accordingly, the 2-indenylidene chloropalladate [ $\{\text{Ind}(\text{Ph}_2\text{P}=\text{S})_2\}\text{PdCl}\}^-$ ] was found to behave as a  $\kappa^2$ -C,S bidentate ligand toward metal fragments, giving access to homo- and heteropolymetallic complexes. X-ray diffraction analyses reveal the presence of short metal–metal contacts in all of these complexes. Density functional theory calculations unambiguously substantiate that the metals engage in unusual  $d^8 \cdots d^8$  interactions with a quasi-perpendicular arrangement of their coordination planes.



Density functional theory calculations unambiguously substantiate that the metals engage in unusual  $d^8 \cdots d^8$  interactions with a quasi-perpendicular arrangement of their coordination planes.

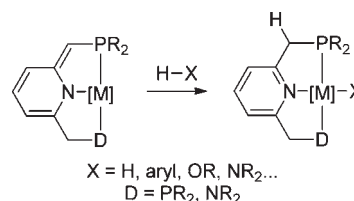
## INTRODUCTION

The last 2 decades have witnessed tremendous developments with pincer complexes.<sup>1</sup> The chelating rigid nature of the involved tridentate ligands imparts a unique balance of stability versus reactivity, which has allowed for spectacular catalytic developments in a variety of transformations. In addition, the ability of the ligand backbone to actively participate in chemical transformations (so-called noninnocent character) has opened up new avenues. Particularly remarkable are the pyridine-based ligands recently developed by Milstein and co-workers. Indeed, metal–ligand cooperation via aromatization/dearomatization confers a new functionality to the pincer scaffold, and thanks to this peculiar behavior, a variety of H–X bonds ( $X = \text{H}$ , aryl, OR,  $\text{NR}_2$ , etc.) can be activated under mild conditions (Chart 1).<sup>2,3</sup>

Inspired by these achievements, we became interested in exploring the coordination properties of tridentate ligands featuring lateral coordination sites prone to acting as bridging ligands, such as sulfur atoms. The ability of a unique pincer ligand to support the coordination of several metals was envisioned to afford original polymetallic species<sup>4</sup> in a straightforward and controlled manner. The association of several metal centers often leads to peculiar chemical and photophysical properties that are relevant to numerous fields including cooperative multicenter catalysis, materials science, and bioinorganic chemistry. Thorough analysis of the bonding situation via modern analytical techniques and computational methods is also of great interest, especially to gain a better understanding of the various types of metal–metal interactions.

Over the past few years, our group has investigated the influence of short donating side arms on the coordination properties of fluorenyl and indenyl moieties.<sup>5,6</sup> In particular, double C–H activation of 1,3-bis(thiophosphinoyl)indene was

**Chart 1. Schematic Representation of H–X Bond Activation with Pincer Complexes Featuring Noninnocent Pyridine-Based Ligands**



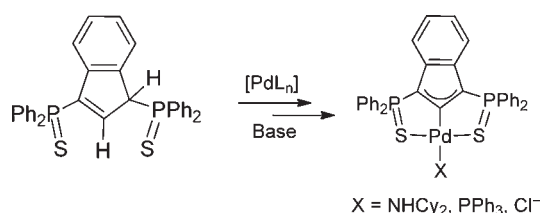
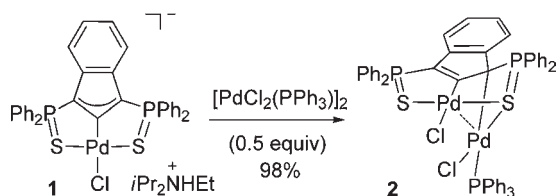
shown to give access to original 2-indenylidene pincer complexes [ $\{\text{Ind}(\text{Ph}_2\text{P}=\text{S})_2\}\text{PdX}\}$  ( $X = \text{NHCy}_2, \text{PPh}_3, \text{Cl}^-$ ; Chart 2).<sup>6</sup> The ability of thiophosphinoyl moieties to act as bridging ligands<sup>7</sup> prompted us to investigate the preparation of polymetallic species from the  $\{\text{Ind}(\text{Ph}_2\text{P}=\text{S})_2\}$  platform,<sup>8</sup> and we report herein homobimetallic (Pd–Pd), heterobimetallic (Pd–Ir), and homotrimetallic (Pd–Pd–Pd) systems. X-ray diffraction analyses reveal the presence of short metal–metal contacts in all of these complexes. Density functional theory (DFT) calculations unambiguously substantiate that the metals engage in unusual  $d^8 \cdots d^8$  interactions with a quasi-perpendicular arrangement of their coordination planes.

## RESULTS AND DISCUSSION

The chloropalladate [ $\{\text{Ind}(\text{Ph}_2\text{P}=\text{S})_2\}\text{PdCl}\}[\text{NHEtPr}_2]$  (**1**)<sup>6a</sup> was first reacted with  $1/2$  equiv of  $[\text{PdCl}_2(\text{PPh}_3)]_2$  at room temperature in dichloromethane (DCM). After stirring overnight

**Received:** April 22, 2011

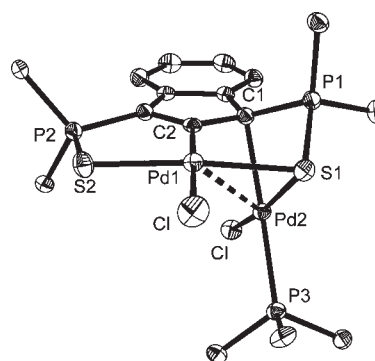
**Published:** June 07, 2011

**Chart 2. Preparation of 2-Indenylidene Pincer Complexes by Double C–H Activation of 1,3-Bis(thiophosphinoyl)indene**

**Scheme 1. Synthesis of the Homobimetallic Complex 2 Starting from the Chloropalladate 1**


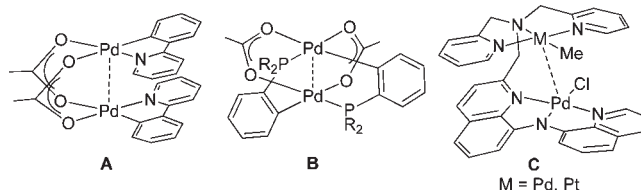
and workup, complex **2** was isolated in excellent yield as a red powder (Scheme 1).<sup>9</sup> <sup>31</sup>P NMR spectroscopy indicates dissymmetrization of the {Ind(Ph<sub>2</sub>P=S)<sub>2</sub>} moiety. The two P=S units are no longer equivalent and resonate in **2** as two doublet signals at 51.0 ppm ( $J = 3.4$  Hz) and 49.4 ppm ( $J = 18.8$  Hz), while a dd signal is found at 28.1 ppm ( $J = 18.8$  and 3.4 Hz) for the PPh<sub>3</sub> ligand at palladium. Also noteworthy is the upfield shift of the <sup>13</sup>C NMR resonance signal associated with C1 (from 104.2 ppm in **1** to 57.6 ppm in **2**), suggesting a change in hybridization from sp<sup>2</sup> to sp<sup>3</sup>.<sup>10</sup>

According to X-ray diffraction analysis (Figure 1), the chloropalladate fragment behaves as a bidentate ligand and coordinates the incoming [PdCl(PPh<sub>3</sub>)] fragment through C1 and the adjacent P=S unit. The C1–P1 bond deviates from the mean indenyl plane by 27° to enable the sulfur atom S1 to bridge the two palladium centers. Both metal atoms adopt square-planar arrangements that are approximately perpendicular to each other ( $\gamma = 88^\circ$ ). Remarkably, the Pd–Pd distance [2.9848(2) Å] is significantly shorter than the sum of the van der Waals radii (4.10 Å)<sup>11a</sup> and exceeds the sum of the covalent radii (2.78 Å)<sup>11b</sup> by only 7%.

The geometric features of complex **2** raise the question about the presence of some Pd···Pd interaction. The ability of d<sup>8</sup> fragments to engage in M···M contacts was recognized early on<sup>12</sup> and is currently attracting growing interest. Unsupported d<sup>8</sup>···d<sup>8</sup> interactions have been observed upon the spontaneous association of ML<sub>4</sub> fragments,<sup>13</sup> but most examples involve short bridging ligands<sup>14</sup> that bring together the metal fragments. Representative examples of palladium-containing complexes featuring d<sup>8</sup>···d<sup>8</sup> interactions are depicted in Chart 3.<sup>15–17</sup> Characteristic features of these complexes are the parallel arrangement of the interacting square-planar d<sup>8</sup> fragments and the short intermetallic distances. As substantiated by computational studies, the d<sup>8</sup>···d<sup>8</sup> interactions are weakly bonding but cannot be considered as genuine chemical bonds. They involve two types of orbital overlaps along the direction perpendicular to the coordination planes: (i) a repulsive four-electron interaction between the filled d<sub>z<sup>2</sup></sub> orbitals of the two fragments and (ii) attractive donor–acceptor interactions between the filled d<sub>z<sup>2</sup></sub> and vacant p<sub>z</sub> orbitals.<sup>12b,14e,15b,c,18</sup>



**Figure 1.** Ellipsoid drawing (50% probability) of the molecular structure of **2**. For clarity, lattice solvent molecules (three CH<sub>2</sub>Cl<sub>2</sub> molecules per asymmetric unit) and hydrogen atoms are omitted and the phenyl groups at phosphorus are simplified.

**Chart 3. Representative Examples of Known Palladium-Containing Polymetallic Complexes Featuring d<sup>8</sup>···d<sup>8</sup> Interactions**


**Table 1.** Selected Geometric Data (Bond Lengths in Angstroms and Angles in Degrees) Determined Experimentally and Computed at the B3PW91/SDD(Pd,Ir,P,S),6-31G\*\*-(Other Atoms) Level of Theory for Complexes **2–4** (M is the Metal Added to **1**)

		Pd–M	$\gamma^a$	Pd–M Wiberg indexes	NBO analysis <sup>b</sup>	
					Pd → M	M → Pd
<b>2</b>	X-ray	2.9848(2)	88			
	DFT	3.13	88	0.11	42	30
<b>3</b>	X-ray	3.0989(4)	96			
	DFT	2.98	97	0.13	13	79
<b>4</b>	X-ray	3.230(2)	100			
	DFT	3.181	97	0.11	13	8

<sup>a</sup> Mean angle between the coordination planes of the two metals.  
<sup>b</sup> Delocalization energy in kcal/mol.

On the one hand, the Pd–Pd distance in **2** is between those observed in complexes **A–C** (2.54–3.19 Å), suggesting the presence of some Pd···Pd interaction. On the other hand, the bridging coordination of the sulfur atom in **2** results in a quasi-perpendicular arrangement of the two palladium coordination planes that markedly contrasts with the usual parallel disposition.<sup>19</sup> To gain deeper insight into the bonding situation in **2**, DFT calculations were carried out at the B3PW91/SDD-(Pd,P,S),6-31G\*\*-(other atoms) level of theory.<sup>20</sup> The optimized geometry of **2** fits nicely with that determined experimentally (Table 1). Close inspection of the molecular orbitals (MOs) combined with natural bond order (NBO) analyses revealed the

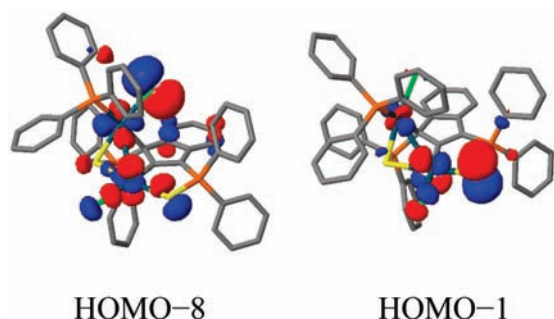
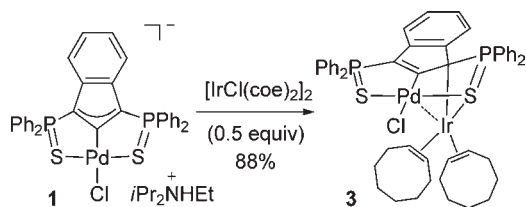


Figure 2. Selected MOs of complex 2.

### Scheme 2. Synthesis of the Heterobimetallic Complex 3



presence of a Pd–Pd interaction reminiscent of that occurring in parallel  $d^8 \cdots d^8$  systems. Among the MOs with strong metal parentages, two filled orbitals with bonding and antibonding Pd–Pd character are present (HOMO–8 and HOMO–1, respectively; Figure 2). In addition, donor–acceptor interactions are found at the second-order perturbation level in the NBO analysis. The different environments of the two palladium centers result in a slightly dissymmetric situation (the delocalization energies corresponding to Pd1  $\rightarrow$  Pd2 and Pd2  $\rightarrow$  Pd1 interactions amount to 42 and 30 kcal/mol, respectively). Despite the perpendicular arrangement of the two coordination planes, the palladium-centered orbitals are diffuse enough to overlap, resulting overall in a weak bonding interaction. Consistently, the Pd–Pd bond order calculated for 2 (Wiberg index = 0.11) is equivalent to that reported for the prototypical parallel system [(2-phenylpyridine)Pd( $\mu$ -OAc)]<sub>2</sub> (0.11).<sup>15b</sup> The presence of a Pd–S–Pd ring critical point in the atom in molecules (AIM) analysis also supports the existence of a Pd–Pd interaction in complex 2.<sup>20</sup>

To evaluate the generality of the synthesis and bonding features of the homobimetallic complex 2, we then targeted a heterobimetallic species. The chloropalladate 1 readily and cleanly reacted with [IrCl(coe)<sub>2</sub>]<sub>2</sub> (coe = cyclooctene) over 2 h at room temperature to give the Pd–Ir complex 3 (88% isolated yield; Scheme 2). Dissymmetrization of the {Ind(Ph<sub>2</sub>P=S)<sub>2</sub>} skeleton was clearly apparent from the <sup>31</sup>P NMR spectrum (two broad signals are found at 50.5 and 49.0 ppm for the two P=S side arms) and the <sup>13</sup>C NMR spectrum (C1 and C3 resonate at 57.9 and 124.8 ppm, respectively). X-ray crystallography substantiated the structural analogy between 2 and 3 (Figure 3). The carbon atom C1 coordinates to the [Ir(coe)<sub>2</sub>] fragment and the adjacent sulfur atom bridges the two metal atoms whose coordination planes are approximately perpendicular ( $\gamma = 96^\circ$ ). A short intermetallic distance is observed [Pd–Ir = 3.0989(4) Å compared with 4.05 Å for the sum of the van der Waals radii and 2.80 Å for the sum of the covalent radii].<sup>11</sup> As for the homobimetallic complex 2, the

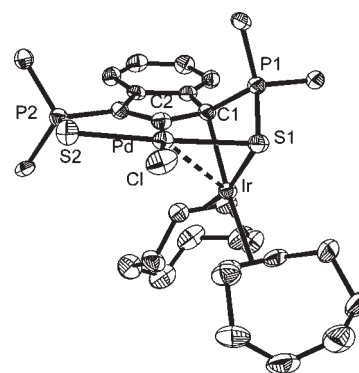
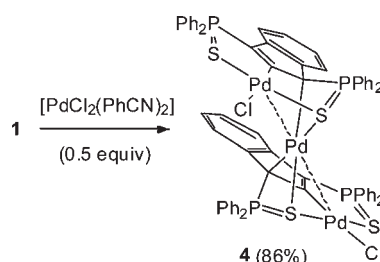


Figure 3. Simplified ellipsoid drawing (50% probability) of the molecular structure of 3. For clarity, lattice solvent molecules (one and a half CH<sub>2</sub>Cl<sub>2</sub> molecules per asymmetric unit) and hydrogen atoms are omitted and the phenyl groups at phosphorus are simplified.

### Scheme 3. Synthesis of the Homotrimetallic Complex 4

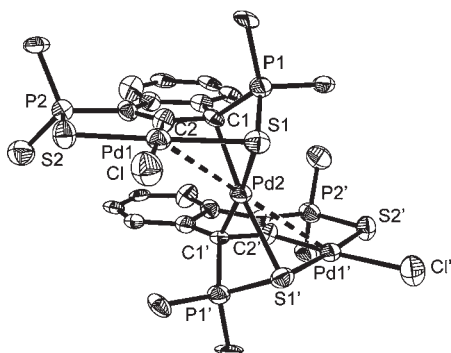


presence of Pd–Ir interaction in 3 was unambiguously corroborated by DFT calculations.<sup>20</sup> The most noticeable difference is the marked dissymmetry of the donor–acceptor interactions in 3: in line with the higher Lewis basicity of Ir<sup>I</sup> over Pd<sup>II</sup>, the Ir  $\rightarrow$  Pd interaction (79 kcal/mol) predominates over the Pd  $\rightarrow$  Ir interaction (13 kcal/mol).

Encouraged by these results, we envisioned the preparation of a trimetallic complex. The chloropalladate 1 was reacted with  $1/2$  equiv of [PdCl<sub>2</sub>(PhCN)<sub>2</sub>] at room temperature in DCM. Over 2 h, the initially orange solution turned to dark red, and complex 4 was isolated in 86% yield after workup (Scheme 3). Extremely low solubility prevented NMR characterization, but the trimetallic structure of 4 was authenticated by X-ray diffraction analysis (Figure 4). Accordingly, a palladium(II) center is entrapped by two chloropalladate fragments that both behave as  $\kappa^2$ -C,S bidentate ligands and arrange in a cis fashion. The coordination plane of the central palladium(II) atom forms an angle of ca. 100° with the outside palladium fragments, which are almost parallel to each other. The Pd<sub>1</sub>–Pd<sub>2</sub> and Pd<sub>2</sub>–Pd<sub>1'</sub> distances [3.231(2) Å] slightly exceed that of 2 but are actually very similar to that found in the homobimetallic complex of type C [3.1909(7) Å].<sup>17</sup> Here also, DFT calculations were carried out and the presence of three-center  $d^8$ – $d^8$ – $d^8$  interaction was apparent from the corresponding MO, NBO, and AIM data.<sup>20</sup>

## CONCLUSIONS

Complexes 3 and 4 represent rare examples of heterobimetallic and trimetallic species featuring  $d^8 \cdots d^8$  interactions,<sup>19,21,22</sup> and their straightforward preparation from the chloropalladate complex 1 substantiates the synthetic potential of pincer complexes in this perspective. Thanks to the bridging ability of the lateral



**Figure 4.** Simplified ellipsoid drawing (50% probability) of the molecular structure of **4**. For clarity, lattice solvent molecules (three  $\text{CH}_2\text{Cl}_2$  molecules per asymmetric unit) and hydrogen atoms are omitted and the phenyl groups at phosphorus are simplified.

thiophosphinoyl donating groups, a unique S–C–S tridentate platform supports the coordination of two metals, leading to original  $d^8 \cdots d^8$  interactions between quasi-perpendicular metal fragments. Ongoing studies aim at taking advantage of the modularity of this strategy to prepare a variety of such polymetallic species. The influence of their peculiar structure on their properties and reactivity is also under investigation.

## EXPERIMENTAL SECTION

**General Considerations.** All reactions and manipulations were carried out under an atmosphere of dry argon using standard Schlenk techniques. Dry, oxygen-free solvents were employed. All organic reagents were obtained from commercial sources and used as received.  $[\text{Pd}(\text{PhCN})_2\text{Cl}_2]$  and  $[\text{IrCl}(\text{coe})_2]_2$  were purchased from STEM.  $[\text{Pd}(\text{PPh}_3)_2\text{Cl}_2]$ ,  $[\text{PdCl}[\text{IndH}(\text{Ph}_2\text{P}=\text{S})_2]]$ ,<sup>23</sup> and  $[\text{PdCl}[\text{Ind}(\text{Ph}_2\text{P}=\text{S})_2]]$  ( $i\text{Pr}_2\text{EtNH}$ )<sup>6</sup> were prepared according to literature procedures.  $^{31}\text{P}$ ,  $^1\text{H}$ , and  $^{13}\text{C}$  NMR spectra were recorded on Bruker Avance 300 or 400 and AMX500 spectrometers.  $^{31}\text{P}$ ,  $^1\text{H}$ , and  $^{13}\text{C}$  chemical shifts are expressed with a positive sign, in parts per million, relative to external 85%  $\text{H}_3\text{PO}_4$  and  $\text{Me}_4\text{Si}$ . Unless otherwise stated, NMR spectra were recorded at 293 K. The  $N$  values corresponding to  $1/2(J_{\text{AX}} + J_{\text{BX}})$  are provided when second-order ABX systems are observed in the  $^{13}\text{C}$  NMR spectra.<sup>24</sup>

**Synthesis of the Homobimetallic Pincer Complex  $\{\text{Pd}[\text{Ind}(\text{Ph}_2\text{P}=\text{S})_2]\text{PdCl}(\text{PPh}_3)\}$  (**2**).** **Method A:** Complex  $\{\text{PdCl}[\text{Ind}(\text{Ph}_2\text{P}=\text{S})_2]\}$  (**1**) was generated in situ by the reaction of  $\{\text{PdCl}[\text{IndH}(\text{Ph}_2\text{P}=\text{S})_2]\}$  (56.5 mg, 0.08 mmol) and  $\text{NEt}_3\text{Pr}_2$  (14  $\mu\text{L}$ , 0.08 mmol) in tetrahydrofuran (THF; 10 mL) at  $-78^\circ\text{C}$ . After stirring at this temperature for 2 h,  $[\text{PdCl}_2(\text{PPh}_3)]_2$  (35.9 mg, 0.04 mmol) in  $\text{CH}_2\text{Cl}_2$  (20 mL) was added, and the reaction mixture was stirred overnight at room temperature. A precipitate was formed by the addition of pentane (40 mL). A dark-red solid was isolated after filtration and drying under vacuum for 1 h. THF (15 mL) was added at  $0^\circ\text{C}$ , and the ammonium salts were removed by filtration. Complex **2** was isolated as a red powder after the solvent was removed under vacuum. **Method B:** An orange suspension containing  $\{\text{PdCl}[\text{IndH}(\text{Ph}_2\text{P}=\text{S})_2]\}$  (56.5 mg, 0.08 mmol),  $[\text{PdCl}_2(\text{PPh}_3)]_2$  (35.9 mg, 0.04 mmol), and 1.5 equiv of polystyrene-supported diisopropylethylamine (PS-DIEA; 42 mg, 0.12 mmol) in  $\text{CH}_2\text{Cl}_2$  (20 mL) was stirred overnight at room temperature. The PS-DIEA·HCl ammonium salts were removed by filtration. Pentane (60 mL) was added to induce precipitation of **2**. Complex **2** was isolated as a red powder (87.5 mg, 98%) after filtration, washing with pentane ( $3 \times 20$  mL), and drying under vacuum. The slow diffusion of  $\text{Et}_2\text{O}$  (40 mL) into a  $\text{CH}_2\text{Cl}_2$  solution of **2** (20 mL) at room temperature

afforded crystals suitable for X-ray diffraction analysis. Mp:  $250^\circ\text{C}$ .  $^{31}\text{P}\{^1\text{H}\}$  NMR (202.5 MHz,  $\text{CDCl}_3$ ):  $\delta$  51.0 (d,  $J_{\text{P,P}} = 3.4$  Hz), 49.4 (d,  $J_{\text{P,P}} = 18.8$  Hz), 28.1 (dd,  $J_{\text{H,P}} = 18.8$  and 3.4 Hz).  $^1\text{H}$  NMR (500 MHz,  $\text{CDCl}_3$ ):  $\delta$  8.56 (dd,  $^3J_{\text{H,P}} = 14.5$  Hz and  $^3J_{\text{H,H}} = 7.0$  Hz, 2H,  $H_{\text{ortho}}\text{PPh}_2$ ), 7.94 (dddd,  $^3J_{\text{H,H}} = 22.5$  Hz,  $^3J_{\text{H,H}} = 12.5$  Hz,  $^4J_{\text{H,P}} = 7.5$  Hz, and  $^4J_{\text{H,H}} = 1.5$  Hz, 4H,  $H_{\text{meta}}\text{PPh}_2$ ), 7.84 (td,  $^3J_{\text{H,H}} = 7.5$  Hz and  $^5J_{\text{H,P}} = 2.0$  Hz, 1H,  $H_{\text{para}}\text{PPh}_2$ ), 7.74 (ddd,  $^3J_{\text{H,P}} = 12.0$  Hz,  $^3J_{\text{H,H}} = 7.0$  Hz, and  $^4J_{\text{H,H}} = 1.0$  Hz, 6H,  $H_{\text{ortho}}\text{PPh}_2$ ), 7.68 (td,  $^3J_{\text{H,H}} = 8.0$  Hz and  $^5J_{\text{H,P}} = 3.5$  Hz, 2H,  $H_{\text{para}}\text{PPh}_2$ ), 7.65 (td,  $^3J_{\text{H,H}} = 9.0$  Hz and  $^5J_{\text{H,P}} = 1.5$  Hz, 1H,  $H_{\text{para}}\text{PPh}_2$ ), 7.57–7.47 (m, 6H,  $H_{\text{ortho}}\text{PPh}_3$ ), 7.42–7.39 (m, 7H,  $H_{\text{meta}}\text{PPh}_2$  and  $H_{\text{para}}\text{PPh}_3$ ), 7.30 (td,  $^3J_{\text{H,H}} = ^3J_{\text{H,H}} = 8.0$  Hz and  $^4J_{\text{H,P}} = 2.5$  Hz, 6H,  $H_{\text{meta}}\text{PPh}_3$ ), 7.19 (d,  $^3J_{\text{H,H}} = 7.5$  Hz, 1H,  $H_6$ ), 7.05 (pt,  $^3J_{\text{H,H}} = ^3J_{\text{H,H}} = 7.5$  Hz, 1H,  $H_5$ ), 7.01 (pseudo-t,  $^3J_{\text{H,H}} = ^3J_{\text{H,H}} = 8.0$  Hz, 1H,  $H_8$ ), 6.94 (td,  $^3J_{\text{H,H}} = 7.5$  Hz and  $^3J_{\text{H,H}} = 1.0$  Hz, 1H,  $H_7$ ).  $^{13}\text{C}\{^1\text{H}\}$  NMR (125.8 MHz,  $\text{CDCl}_3$ ):  $\delta$  162.39 (ddd,  $^2J_{\text{C,P}} = 28.1$  Hz,  $^2J_{\text{C,P}} = 17.7$  Hz, and  $^2J_{\text{C,P}} = 3.6$  Hz,  $\text{C}_2$ ), 145.41 (ddd,  $^2J_{\text{C,P}} = 18.0$  Hz,  $^3J_{\text{C,P}} = 9.6$  Hz, and  $^4J_{\text{C,P}} = 2.7$  Hz,  $\text{C}_4$ ), 140.99 (d pseudo-t,  $^2J_{\text{C,P}} = 10.9$  Hz and  $^3J_{\text{C,P}} = ^3J_{\text{C,P}} = 4.5$  Hz,  $\text{C}_9$ ), 134.89 (d,  $^2J_{\text{C,P}} = 12.7$  Hz,  $\text{C}_{\text{ortho}}$ ), 134.60 (d,  $^3J_{\text{C,P}} = 11.3$  Hz,  $\text{C}_{\text{meta}}\text{PPh}_3$ ), 134.38 (d,  $^4J_{\text{C,P}} = 2.9$  Hz,  $\text{C}_{\text{para}}$ ), 133.65 (d,  $^4J_{\text{C,P}} = 3.1$  Hz,  $\text{C}_{\text{para}}$ ), 132.86 (d,  $^2J_{\text{C,P}} = 11.6$  Hz,  $\text{C}_{\text{meta}}$ ), 132.60 (d,  $^3J_{\text{C,P}} = 11.4$  Hz,  $\text{C}_{\text{meta}}$ ), 132.64 (d,  $^1J_{\text{C,P}} = 65.5$  Hz,  $\text{C}_{\text{ipso}}$ ), 132.51 (d,  $^4J_{\text{C,P}} = 2.9$  Hz,  $\text{C}_{\text{para}}$ ), 132.33 (d,  $^4J_{\text{C,P}} = 3.0$  Hz,  $\text{C}_{\text{para}}$ ), 130.96 (d,  $^4J_{\text{C,P}} = 2.6$  Hz,  $\text{C}_{\text{para}}\text{PPh}_3$ ), 130.14 (d,  $^1J_{\text{C,P}} = 81.5$  Hz,  $\text{C}_{\text{ipso}}$ ), 129.86 (d,  $^3J_{\text{C,P}} = 11.4$  Hz,  $\text{C}_{\text{meta}}$ ), 129.76 (d,  $^1J_{\text{C,P}} = 62.2$  Hz,  $\text{C}_{\text{ipso}}\text{PPh}_3$ ), 129.75 (d,  $^4J_{\text{C,P}} = 50.3$  Hz,  $\text{C}_{\text{ipso}}$ ), 129.66 (d,  $^2J_{\text{C,P}} = 12.7$  Hz,  $\text{C}_{\text{ortho}}$ ), 129.46 (d,  $^2J_{\text{C,P}} = 13.1$  Hz,  $\text{C}_{\text{ortho}}$ ), 129.19 (d,  $^2J_{\text{C,P}} = 13.1$  Hz,  $\text{C}_{\text{ortho}}$ ), 128.81 (d,  $^2J_{\text{C,P}} = 12.6$  Hz,  $\text{C}_{\text{meta}}$ ), 128.75 (d,  $^3J_{\text{C,P}} = 11.1$  Hz,  $\text{C}_{\text{ortho}}\text{PPh}_3$ ), 126.09 ( $^1J_{\text{C,P}} = 83.4$  Hz,  $\text{C}_{\text{ipso}}$ ), 125.12 ( $\text{C}_5$ ), 124.95 (ddd,  $^1J_{\text{C,P}} = 131.4$  Hz,  $^3J_{\text{C,P}} = 13.7$  Hz, and  $^3J_{\text{C,P}} = 1.0$  Hz,  $\text{C}_3$ ), 121.75 ( $\text{C}_7$ ), 121.40 ( $\text{C}_6$ ), 118.34 ( $\text{C}_8$ ), 57.65 (ddd,  $^1J_{\text{C,P}} = 81.1$  Hz,  $^2J_{\text{C,P}} = 63.8$  Hz, and  $^3J_{\text{C,P}} = 17$  Hz,  $\text{C}_1$ ). Calcd for  $\text{C}_{51}\text{H}_{40}\text{ClP}_3\text{Pd}_2\text{S}_2$ : C, 56.06; H, 3.60; S, 5.87. Found: C, 55.91; H, 3.73; S, 5.57. HRMS (ESI). Calcd for  $2$  ( $\text{C}_{51}\text{H}_{39}\text{Cl}_2\text{P}_3\text{Pd}_2\text{S}_2$ ): 1089.9153. Calcd for  $[\text{M} - \text{Cl}]^+$  ( $\text{C}_{51}\text{H}_{39}\text{ClP}_3\text{Pd}_2\text{S}_2$ ): 1054.94641. Found: 1054.9490.

**Synthesis of the Heterobimetallic Pincer Complex  $\{\text{Pd}[\text{Ind}(\text{Ph}_2\text{P}=\text{S})_2]\text{Ir}(\text{coe})_2\}$  (**3**).** **Method A:** Complex **1** was generated in situ by the reaction of  $\{\text{PdCl}[\text{IndH}(\text{Ph}_2\text{P}=\text{S})_2]\}$  (56.5 mg, 0.08 mmol) and  $\text{NEt}_3\text{Pr}_2$  (14  $\mu\text{L}$ , 0.08 mmol) in THF (10 mL) at  $-78^\circ\text{C}$ . After stirring at this temperature for 2 h,  $[\text{IrCl}(\text{coe})_2]_2$  (27.7 mg, 0.04 mmol) in  $\text{CH}_2\text{Cl}_2$  (20 mL) was added and the reaction mixture was stirred overnight at room temperature. An orange solid was obtained after precipitation with pentane (40 mL), filtration, and drying under vacuum for 1 h. THF (15 mL) was added at  $0^\circ\text{C}$ , and the ammonium salts were removed by filtration. Complex **3** was isolated as a red powder from the supernatant, after the solvent was removed under vacuum. **Method B:** An orange suspension containing  $\{\text{PdCl}[\text{IndH}(\text{Ph}_2\text{P}=\text{S})_2]\}$  (56.5 mg, 0.08 mmol),  $[\text{IrCl}(\text{coe})_2]_2$  (27.7 mg, 0.04 mmol), and 1.5 equiv of PS-DIEA (42 mg, 0.12 mmol) in  $\text{CH}_2\text{Cl}_2$  (15 mL) was stirred at room temperature for 2 h. The PS-DIEA·HCl ammonium salts were removed by filtration. Pentane (60 mL) was added to induce precipitation. Complex **3** was isolated as a red powder (79.2 mg, 88%) after filtration, washing with pentane ( $3 \times 20$  mL), and drying under vacuum. The slow diffusion of pentane (40 mL) into a  $\text{CH}_2\text{Cl}_2$  solution of **3** (20 mL) at room temperature afforded crystals suitable for X-ray diffraction analysis. Mp:  $346^\circ\text{C}$  (dec).  $^{31}\text{P}\{^1\text{H}\}$  NMR (202.5 MHz,  $\text{CDCl}_3$ ):  $\delta$  50.6 (br), 49.0 (br).  $^1\text{H}$  NMR (500 MHz,  $\text{CDCl}_3$ ):  $\delta$  8.74 (dd,  $^3J_{\text{H,P}} = 13.0$  Hz and  $^3J_{\text{H,H}} = 7.5$  Hz, 2H,  $H_{\text{ortho}}\text{PPh}_2$ ), 8.08 (dd,  $^4J_{\text{H,P}} = 11.5$  Hz and  $^3J_{\text{H,H}} = 7.0$  Hz, 2H,  $H_{\text{meta}}\text{PPh}_2$ ), 7.82 (t,  $^3J_{\text{H,H}} = 6.5$  Hz, 1H,  $H_{\text{para}}\text{PPh}_2$ ), 7.70–7.61 (m, 5H,  $2H_{\text{ortho}}\text{PPh}_2$ ,  $2H_{\text{meta}}\text{PPh}_2$ , and  $H_{\text{para}}\text{PPh}_2$ ), 7.54 (br, 4H,  $2H_{\text{ortho}}\text{PPh}_2$  and  $2H_{\text{para}}\text{PPh}_2$ ), 7.43 (pseudo-t,  $^3J_{\text{H,H}} = ^3J_{\text{H,P}} = 6.6$  Hz, 2H,  $2H_{\text{ortho}}\text{PPh}_2$ ), 7.33 (pseudo-t,  $^3J_{\text{H,H}} = ^3J_{\text{H,H}} = 7.0$  Hz, 2H,  $2H_{\text{meta}}\text{PPh}_2$ ), 7.04 (br, 4H,  $H_5$ ,  $H_8$ , and  $2H_{\text{meta}}\text{PPh}_2$ ), 6.80 (pt,  $^3J_{\text{H,H}} = ^3J_{\text{H,H}} = 6.5$  Hz, 1H,  $H_6$ ), 6.64 (d,  $^3J_{\text{H,H}} = 6.0$  Hz, 1H,  $H_7$ ), 3.59 (d,  $^3J_{\text{H,H}} = 8.5$  Hz, 1H, =CH), 3.50 (m, 1H, =CH), 3.13 (m, 2H, =CH), 2.45 (br, 1H,  $\text{CH}_2$ ), 2.39 (d,  $J_{\text{H,H}} = 15.0$  Hz, 1H,  $\text{CH}_2$ ),

2.24 (d,  $J_{\text{H,H}} = 13.0$  Hz, 1H,  $\text{CH}_2$ ), 1.86 (br, 1H,  $\text{CH}_2$ ), 1.80 (d,  $J_{\text{H,H}} = 13.0$  Hz, 2H,  $\text{CH}_2$ ), 1.71 (br, 1H,  $\text{CH}_2$ ), 1.52 (br, 4H,  $\text{CH}_2$ ), 1.41 (br, 4H,  $\text{CH}_2$ ), 1.28 (br, 2H,  $\text{CH}_2$ ), 1.10 (br, 3H,  $\text{CH}_2$ ), 0.81 (br, 4H,  $\text{CH}_2$ ).  $^{13}\text{C}\{^1\text{H}\}$  NMR (125.8 MHz,  $\text{CDCl}_3$ ):  $\delta$  154.91 (ABX system,  $J = 20.8$  Hz,  $\text{C}_2$ ), 146.30 (dd,  $^2J_{\text{C,P}} = 18.6$  Hz and  $^3J_{\text{C,P}} = 6.6$  Hz,  $\text{C}_4$ ), 137.85 (dd,  $^2J_{\text{C,P}} = 14.2$  and  $^3J_{\text{C,P}} = 10.8$  Hz,  $\text{C}_9$ ), 137.59 (d,  $^2J_{\text{C,P}} = 61.9$  Hz,  $\text{C}_{\text{ipso}}$ ), 135.67 (d,  $^3J_{\text{C,P}} = 13.3$  Hz,  $\text{C}_{\text{ortho}}$ ), 133.94 (d,  $^4J_{\text{C,P}} = 0.5$  Hz,  $\text{C}_{\text{para}}$ ), 133.12 (d,  $^4J_{\text{C,P}} = 2.0$  Hz,  $\text{C}_{\text{para}}$ ), 132.35 ( $\text{C}_{\text{para}}$ ), 132.29 ( $\text{C}_{\text{para}}$ ), 132.27 (d,  $^3J_{\text{C,P}} = 11.3$  Hz,  $\text{C}_{\text{meta}}$ ), 131.95 (d,  $^3J_{\text{C,P}} = 11.4$  Hz,  $\text{C}_{\text{meta}}$ ), 130.60 (d,  $^1J_{\text{C,P}} = 82.8$  Hz,  $\text{C}_{\text{ipso}}$ ), 129.32 (d,  $^1J_{\text{C,P}} = 84.0$  Hz,  $\text{C}_{\text{ipso}}$ ), 129.23 (d,  $^3J_{\text{C,P}} = 10.9$  Hz,  $\text{C}_{\text{meta}}$ ), 129.13 (d,  $^2J_{\text{C,P}} = 13.0$  Hz,  $\text{C}_{\text{meta}}$ ), 128.93 (d,  $^2J_{\text{C,P}} = 13.0$  Hz,  $2\text{C}_{\text{ortho}}$ ), 128.81 (d,  $^2J_{\text{C,P}} = 14.7$  Hz,  $\text{C}_{\text{ortho}}$ ), 125.40 (d,  $^1J_{\text{C,P}} = 82.0$  Hz,  $\text{C}_{\text{ipso}}$ ), 125.25 ( $\text{C}_5$ ), 124.80 (dd,  $^1J_{\text{C,P}} = 64.9$  Hz and  $^3J_{\text{C,P}} = 12.3$  Hz,  $\text{C}_3$ ), 121.70 ( $\text{C}_7$ ), 120.85 ( $\text{C}_6$ ), 117.70 ( $\text{C}_8$ ), 69.59 (=CH), 67.18 (=CH), 59.04 (=CH), 57.95 (dd,  $^1J_{\text{C,P}} = 77.5$  Hz and  $^3J_{\text{C,P}} = 15.7$  Hz,  $\text{C}_1$ ), 54.70 (=CH), 34.69 ( $\text{CH}_2$ ), 33.61 ( $\text{CH}_2$ ), 32.21 ( $\text{CH}_2$ ), 31.32 ( $\text{CH}_2$ ), 29.54 ( $\text{CH}_2$ ), 29.39 ( $\text{CH}_2$ ), 26.70 ( $\text{CH}_2$ ), 26.48 ( $2\text{CH}_2$ ), 26.33 ( $\text{CH}_2$ ), 25.89 ( $\text{CH}_2$ ), 25.55 ( $\text{CH}_2$ ). HRMS (ESI). Calcd for 3 ( $\text{C}_{49}\text{H}_{52}\text{ClIrP}_2\text{PdS}_2$ ): 1100.1338. Calcd for  $[\text{M} - \text{Cl}]^+$  ( $\text{C}_{49}\text{H}_{52}\text{IrP}_2\text{PdS}_2$ ): 1065.1650. Found: 1065.1647.

**Synthesis of the Homotrimetallic Pincer Complex  $\{\text{Pd}_3[\text{Ind}(\text{Ph}_2\text{P}=\text{S})_2]_2\}$  (4).** An orange suspension containing  $\{\text{PdCl}[\text{IndH}(\text{Ph}_2\text{P}=\text{S})_2]\}$  (56.5 mg, 0.08 mmol),  $[\text{PdCl}_2(\text{PhCN})_2]$  (15.8 mg, 0.04 mmol), and PS-DIEA (42 mg, 0.12 mmol) in  $\text{CH}_2\text{Cl}_2$  (15 mL) was stirred at room temperature for 2 h. The PS-DIEA·HCl ammonium salts were removed by filtration, and the resulting dark-red solution was cooled to  $-30$  °C for 12 h. Dark-red crystals of 4 were isolated (52.1 mg, 86%) after filtration. Mp: 344 °C (dec). HRMS (ESI). Calcd for 4 ( $\text{C}_{66}\text{H}_{48}\text{Cl}_2\text{P}_4\text{Pd}_3\text{S}_4$ ): 1479.8071. Calcd for  $[\text{M} - \text{Cl}]^+$  ( $\text{C}_{66}\text{H}_{48}\text{Cl}_2\text{P}_4\text{Pd}_3\text{S}_4$ ): 1444.8382. Found: 1444.8404. Complex 4 is insoluble in all of the typical NMR solvents, preventing NMR characterization.

**X-ray Crystallography and Data Collection.** Crystallographic data (excluding structure factors) have been deposited to the Cambridge Crystallographic Data Centre as supplementary publication nos. CCDC 812443 (2), 812444 (3), and 812445 (4). These data can be obtained free of charge via [www.ccdc.cam.ac.uk/conts/retrieving.html](http://www.ccdc.cam.ac.uk/conts/retrieving.html) (or from the CCDC, 12 Union Road, Cambridge CB2 1EZ, U.K.; fax (+44) 1223-336-033 or e-mail [deposit@ccdc.cam.ac.uk](mailto:deposit@ccdc.cam.ac.uk)).

The data for compounds 2–4 were collected on a Bruker-AXS SMART APEX II diffractometer at temperatures of 173(2) K (2), 193(3) K (3), and 233(4) K (4) using an oil-coated shock-cooled crystal with graphite-monochromated Mo  $K\alpha$  radiation (wavelength = 0.71073 Å) by using  $\varphi$  and  $\omega$  scans. The data were integrated with SAINT, and an empirical absorption correction with SADABS was applied.<sup>25,26</sup> The structures were solved by direct methods (SHELXS-97),<sup>27</sup> and refined against all data by the full-matrix least-squares methods on  $F^2$  (SHELXL-97).<sup>28</sup> All non-hydrogen atoms were refined with anisotropic displacement parameters. The hydrogen atoms were refined isotropically on calculated positions using a riding model, with their  $U_{\text{iso}}$  values constrained to  $1.5U_{\text{eq}}$  of their pivot atoms for terminal  $\text{sp}^3$  carbon atoms and 1.2 times for all other carbon atoms. The crystals of 4 proved extremely unstable out of solution whatever the temperature. This complicated the X-ray diffraction analysis and explains the low completeness (91.6%). The optimal temperature for data collection was found to be 233 K (faster decomposition was observed at room temperature as well as 193 K). Complexes 2–4 were obtained as solvates, and the methylene chloride molecules were disordered. Geometrical restraint (SAME), similar ADP (anisotropic displacement parameter) restraint (SIMU), and rigid-bond restraint (DELU) have been used to make the ADP values of the disordered atoms more reasonable.

2:  $\text{C}_{51}\text{H}_{39}\text{Cl}_2\text{P}_3\text{Pd}_2\text{S}_2 \cdot 3\text{CH}_2\text{Cl}_2$ ,  $M = 1347.33$ , monoclinic, space group  $P2_1/n$ ,  $a = 18.7145(4)$  Å,  $b = 14.7029(3)$  Å,  $c = 21.6880(5)$  Å,  $\beta = 113.9870(10)^\circ$ ,  $\alpha = \gamma = 90^\circ$ ,  $V = 5452.2(2)$  Å<sup>3</sup>,  $Z = 4$ , crystal size

$0.80 \times 0.50 \times 0.02$  mm<sup>3</sup>, 76 301 reflections collected (13 989 independent,  $R_{\text{int}} = 0.0407$ ), 706 parameters, 105 restraints,  $R1 [I > 2\sigma(I)] = 0.0265$ ,  $wR2 [\text{all data}] = 0.0661$ , largest difference peak and hole 0.533 and  $-0.529$  e/Å<sup>3</sup>.

3:  $\text{C}_{49}\text{H}_{47}\text{ClIrP}_2\text{PdS}_2 \cdot 1.5\text{CH}_2\text{Cl}_2$ ,  $M = 1223.36$ , triclinic, space group  $P\bar{1}$ ,  $a = 11.7880(2)$  Å,  $b = 12.6618(2)$  Å,  $c = 18.9211(3)$  Å,  $\alpha = 91.6460(10)^\circ$ ,  $\beta = 106.2320(10)^\circ$ ,  $\gamma = 112.5190(10)^\circ$ ,  $V = 2475.26(7)$  Å<sup>3</sup>,  $Z = 2$ , crystal size  $0.21 \times 0.12 \times 0.04$  mm<sup>3</sup>, 34 279 reflections collected (10 041 independent,  $R_{\text{int}} = 0.0499$ ), 587 parameters, 36 restraints,  $R1 [I > 2\sigma(I)] = 0.0342$ ,  $wR2 [\text{all data}] = 0.0803$ , largest difference peak and hole 0.976 and  $-0.685$  e/Å<sup>3</sup>.

4:  $\text{C}_{66}\text{H}_{48}\text{Cl}_2\text{P}_4\text{Pd}_3\text{S}_4 \cdot 6\text{CH}_2\text{Cl}_2$ ,  $M = 996.41$ , monoclinic, space group  $C2/c$ ,  $a = 34.423(7)$  Å,  $b = 14.298(3)$  Å,  $c = 22.074(4)$  Å,  $\beta = 129.45(3)^\circ$ ,  $\alpha = \gamma = 90^\circ$ ,  $V = 8389(3)$  Å<sup>3</sup>,  $Z = 4$ , crystal size  $0.15 \times 0.05 \times 0.05$  mm<sup>3</sup>, 11 066 reflections collected (6551 independent,  $R_{\text{int}} = 0.1741$ ), 522 parameters, 187 restraints,  $R1 [I > 2\sigma(I)] = 0.0690$ ,  $wR2 [\text{all data}] = 0.1733$ , largest difference peak and hole 0.928 and  $-0.736$  e/Å<sup>3</sup>.

## ■ ASSOCIATED CONTENT

Supporting Information. Computational details and crystallographic data (CIF) for compounds 2–4. This material is available free of charge via the Internet at <http://pubs.acs.org>.

## ■ AUTHOR INFORMATION

### Corresponding Author

\*E-mail: [dbouriss@chimie.ups-tlse.fr](mailto:dbouriss@chimie.ups-tlse.fr). Tel: +33 (0)5 61 55 77 37. Fax: +33 (0)5 61 55 82 04.

## ■ ACKNOWLEDGMENT

We are grateful to the CNRS, UPS, and COST action CM0802 PhoSciNet for financial support of this work. CalMip (CNRS, Toulouse, France) is acknowledged for calculation facilities. L.M. thanks the Institut Universitaire de France, and N.N. thanks the Ministry of Ciencia e Innovación of Spain for a postdoctoral fellowship. This manuscript is dedicated to the memory of Pascal Le Floch.

## ■ REFERENCES

- (1) (a) Van der Boom, M. E.; Milstein, D. *Chem. Rev.* **2003**, *103*, 1759–1792. (b) *The Chemistry of Pincer Ligands*; Morales-Morales, D., Jensen, C. M., Eds.; Elsevier: Oxford, U.K., 2007. (c) Benito-Garagorri, D.; Kirchner, K. *Acc. Chem. Res.* **2008**, *41*, 201–213.
- (2) (a) Ben-Ari, E.; Leitens, G.; Shimon, L. J. W.; Milstein, D. *J. Am. Chem. Soc.* **2006**, *128*, 15390–15391. (b) Gunanathan, C.; Ben-David, Y.; Milstein, D. *Science* **2007**, *317*, 790–792. (c) Kohl, S. W.; Weiner, L.; Schwartsburd, L.; Konstantinovskii, L.; Shimon, L. J. W.; Ben-David, Y.; Iron, M. A.; Milstein, D. *Science* **2009**, *324*, 74–77. (d) Gnanaprakasam, B.; Zhang, J.; Milstein, D. *Angew. Chem., Int. Ed.* **2010**, *49*, 1468–1471. (e) Khaskin, E.; Iron, M. A.; Shimon, L. J. W.; Zhang, J.; Milstein, D. *J. Am. Chem. Soc.* **2010**, *132*, 8542–8543.
- (3) For recent reviews, see: (a) van der Vlugt, J. I.; Reek, J. N. H. *Angew. Chem., Int. Ed.* **2009**, *48*, 8832–8846. (b) Milstein, D. *Top. Catal.* **2010**, *53*, 915–923.
- (4) (a) *The Chemistry of Metal Clusters*; Shriver, D. F., Kaesz, H. D., Adams, R. D., Eds.; VCH: New York, 1990. (b) *Metal Clusters in Chemistry*; Braunstein, P., Oro, L. A., Raithby, P. R., Eds.; Wiley-VCH: Weinheim, Germany, 1999.
- (5) (a) Freund, C.; Barros, N.; Gornitzka, H.; Martin-Vaca, B.; Maron, L.; Bourissou, D. *Organometallics* **2006**, *25*, 4927–4930. (b) Oulié, P.; Freund, C.; Martin-Vaca, B.; Maron, L.; Bourissou, D. *Organometallics* **2007**, *26*, 6793–6804.

(6) (a) Oulié, P.; Nebra, N.; Saffon, N.; Maron, L.; Martin-Vaca, B.; Bourissou, D. *J. Am. Chem. Soc.* **2009**, *131*, 3493–3498. (b) Nebra, N.; Lisena, J.; Ladeira, S.; Saffon, N.; Maron, L.; Martin-Vaca, B.; Bourissou, D. *Dalton Trans.* **2011**, DOI: 10.1039/c1dt10118h.

(7) For recent examples of bridging coordination involving thiophosphinoyl groups, see: (a) Cantat, T.; Ricard, L.; Le Floch, P.; Mézailles, N. *Organometallics* **2006**, *25*, 4965–4976. (b) Konu, J.; Chivers, T. *Chem. Commun.* **2008**, 4995–4997. (c) Cantat, T.; Arliguie, T.; Noël, A.; Thuéry, P.; Ephritikhine, M.; Le Floch, P.; Mézailles, N. *J. Am. Chem. Soc.* **2009**, *131*, 963–972.

(8) A palladium pincer complex derived from a bis(phosphino)-carbodiphosphorane was recently used to support an original Pd–Au  $d^8 \cdots d^{10}$  pseudo-closed-shell interaction. Reitsamer, C.; Schuh, W.; Kopacka, H.; Wurst, K.; Peringer, P. *Organometallics* **2009**, *28*, 6617–6620.

(9) From a practical viewpoint, in situ generation of the chloropal-ladate **1** by treatment of the  $[\{\text{IndH}(\text{Ph}_2\text{P}=\text{S})_2\}\text{PdCl}]$  precursor with polystyrene-supported diisopropylethylamine proved to facilitate the workup and isolation of **2**.

(10) In the cyclometalated complex  $[\{\text{IndH}(\text{Ph}_2\text{P}=\text{S})_2\}\text{PdCl}(\text{PPh}_3)]$ , C1 resonates at 30.6 ppm.<sup>6b</sup>

(11) (a) Batsanov, S. S. *Inorg. Mater.* **2001**, *37*, 871. (b) Cordero, B.; Gómez, V.; Pletro-Prats, A. E.; Revés, M.; Echeverría, J.; Cremades, E.; Barragán, F.; Alvarez, S. *Dalton Trans.* **2008**, 2832–2838.

(12) (a) Osborn, R. S.; Rogers, D. J. *Chem. Soc., Dalton Trans.* **1974**, 1002–1004. (b) Mann, K. R.; Gordon, J. G., II; Gray, H. B. *J. Am. Chem. Soc.* **1975**, *97*, 3553–3555.

(13) (a) Mann, K. R.; Lewis, N. S.; Williams, R. M.; Gray, H. B.; Gordon, J. G., II *Inorg. Chem.* **1978**, *17*, 828–834. (b) Connick, W. B.; Marsh, R. E.; Schaefer, W. P.; Gray, H. B. *Inorg. Chem.* **1997**, *36*, 913–922. (c) Tran, N. T.; Stork, J. R.; Pham, D.; Olmstead, M. M.; Fetting, J. C.; Balch, A. L. *Chem. Commun.* **2006**, 1130–1132. (d) Lum, W.; Chui, S. S.-Y.; Ng, K.-M.; Che, C.-M. *Angew. Chem., Int. Ed.* **2008**, *47*, 4568–4572. (e) Klerman, Y.; Ben-Ari, E.; Diskin-Posner, Y.; Leitius, G.; Shimon, L. J. W.; Den-David, Y.; Milstein, D. *Dalton Trans.* **2008**, 3226–3234.

(14) (a) Roundhill, D. M.; Gray, H. B.; Che, C.-M. *Acc. Chem. Res.* **1989**, *22*, 55–61. (b) Che, C.-M.; Yam, V. W.-W.; Wong, W.-T.; Lai, T.-F. *Inorg. Chem.* **1989**, *28*, 2908–2910. (c) Yip, H.-K.; Lai, T.-F.; Che, C.-M. *J. Chem. Soc., Dalton Trans.* **1991**, 1639–1641. (d) Xia, B.-H.; Che, C.-M.; Phillips, D. L.; Leung, K.-H.; Cheung, K.-K. *Inorg. Chem.* **2002**, *41*, 3866–3875. (e) Xia, B.-H.; Che, C.-M.; Zhou, Z.-Y. *Chem.—Eur. J.* **2003**, *9*, 3055–3064. (f) Pan, Q.-J.; Zhang, H.-X.; Zhou, X.; Fu, H.-G.; Yu, H.-T. *J. Phys. Chem. A* **2007**, *111*, 287–294. (g) Kim, M.; Taylor, T. J.; Gabbai, F. P. *J. Am. Chem. Soc.* **2008**, *130*, 6332–6333. (h) Powers, D. C.; Ritter, T. *Nat. Chem.* **2009**, *1*, 302–309. (i) Powers, D. C.; Benitez, D.; Tkatchouk, E.; Goddard, W. A., III; Ritter, T. *J. Am. Chem. Soc.* **2010**, *132*, 14092–14103. (j) Powers, D. C.; Xiao, D. Y.; Geibel, M. A. L.; Ritter, T. *J. Am. Chem. Soc.* **2010**, *132*, 14530–14536.

(15) (a) Thu, H.-Y.; Yu, W.-Y.; Che, C.-M. *J. Am. Chem. Soc.* **2006**, *128*, 9048–9049. (b) Bercaw, J. E.; Durell, A. C.; Gray, H. B.; Green, J. C.; Hazari, N.; Labinger, J. A.; Winkler, J. R. *Inorg. Chem.* **2010**, *49*, 1801–1810. (c) Marino, N.; Fazen, C. H.; Blakemore, J. D.; Incarvito, C. D.; Hazari, N.; Doyle, R. P. *Inorg. Chem.* **2011**, *50*, 2507–2520.

(16) (a) Koshevoy, I. O.; Lahuerta, P.; Sanaú, M.; Ubeda, M. A.; Doménech, A. *Dalton Trans.* **2006**, 5536–5541. (b) Bonet, A.; Gulyás, H.; Koshevoy, I. O.; Estevan, F.; Sanaú, M.; Ubeda, M. A.; Fernández, E. *Chem.—Eur. J.* **2010**, *16*, 6382–6390.

(17) Site-selective metallation of polyfunctional ligands combining several bonding motifs gave access to homometallic as well as heterobimetallic species of type C: Suess, D. L. M.; Peters, J. C. *Chem. Commun.* **2010**, 46, 6554–6556.

(18) (a) Novoa, J. J.; Aullón, G.; Alemany, P.; Alvarez, S. *J. Am. Chem. Soc.* **1995**, *117*, 7169–7171. (b) Aullón, G.; Alvarez, S. *Chem.—Eur. J.* **1997**, *3*, 655–664.

(19) The presence of  $d^8 \cdots d^8$  interactions has been suggested in  $\mu_3$ -sulfotriangulopalladium and platinum complexes. See: Tzeng, B.-C.; Chan, S.-C.; Chan, M. C. W.; Che, C.-M.; Cheung, K.-K.; Peng, S.-M.

*Inorg. Chem.* **2001**, *40*, 6699–6704. It has also been suggested in bis( $\mu_2$ -aziridinato)rhodium and -iridium complexes. See: Tejel, C.; Ciriano, M. A.; Passarelli, V.; López, J. A.; de Bruin, B. *Chem.—Eur. J.* **2008**, *14*, 10985–10998.

(20) See the Supporting Information for details.

(21) For a diphosphinomethane-bridged heterobimetallic Pt–Rh complex, see: Yip, H.-K.; Lin, H.-M.; Wang, Y.; Che, C.-M. *Inorg. Chem.* **1993**, *32*, 3402–3407.

(22) For homotrimetallic rhodium and palladium species, see ref 14c and the following: Bercaw, J. E.; Day, M. W.; Golisz, S. R.; Hazari, N.; Henling, L. M.; Labinger, J. A.; Schofer, S. J.; Virgil, S. *Organometallics* **2009**, *28*, 5017–5024.

(23) Noskowska, M.; Sliwinska, E.; Duczmal, W. *Trans. Met. Chem.* **2003**, *28*, 756–759.

(24) (a) *Nuclear Magnetic Resonance Spectroscopy*; Bovey, F. A., Ed.; Academic Press: New York, 1969. (b) Abraham, R. J.; Berstein, H. *Can. J. Chem.* **1961**, *39*, 216–230.

(25) SAINT-NT; Bruker AXS Inc.: Madison, WI, 2000.

(26) SADABS, Program for data correction; Bruker AXS: Madison, WI.

(27) Sheldrick, G. M. *Acta Crystallogr.* **1990**, *A46*, 467–473.

(28) Sheldrick, G. M. *Acta Crystallogr., Sect. A* **2008**, *64*, 112–122.